Reliability Engineering and System Safety 224 (2022) 108536

Contents lists available at ScienceDirect

Reliability Engineering and System Safety

journal homepage: www.elsevier.com/locate/ress

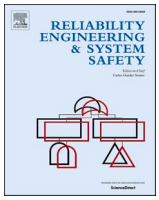

Network hardening and optimal placement of microgrids to improve transmission system resilience: A two-stage linear program

Kamran Jalilpoor [a], Arman Oshnoei [a,d], Behnam Mohammadi-Ivatloo [b,c], Amjad Anvari-Moghaddam [d,*]

[a] Department of Electrical Engineering, Shahid Beheshti University, Tehran, Iran
[b] Faculty of Electrical and Computer Engineering, University of Tabriz, Tabriz, Iran
[c] Information Technologies Application and Research Center, İstanbul Ticaret University, Istanbul, Turkey
[d] Department of Energy (AAU Energy), Aalborg University, 9220 Aalborg, Denmark

ARTICLE INFO

Keywords:
Transmission System Resilience
Natural Phenomenon
Microgrids
Network Hardening

ABSTRACT

This paper aims to develop a linear two-stage optimization problem based on an attacker-defender resilient planning (AD-RP) model to improve the power system's operational and infrastructural resilience in the face of low-probability high-impact events. In the developed model, attackers are natural phenomena that can cause the most severe damage to system performance, and defenders are actions that minimize system vulnerabilities. In the first stage, a stochastic model depending on Monte-Carlo simulation is developed to present a new index for selecting the most vulnerable transmission system components. This index is designed based on combining the worst possible case of attack, disaster statistical analysis, system structure and fragility curves. In the second stage, as defense operations, the hardening of vulnerable lines and microgrids placement in the proper places are carried out considering investment budget constraints. Minimizing load shedding and ensuring the resilience of the transmission network are the main objectives behind the second stage. In this regard, a comprehensive metric for the evaluation of the transmission system resilience is introduced. Thanks to a mixed-integer programming problem, the effectiveness of the proposed AD-RP model in increasing system resilience is demonstrated in the IEEE 30-bus and 118-bus test systems.

1. Introduction

Following technical problems, man-made outages, and natural disasters, a power system may encounter a critical situation or a blackout. Among them all, the role of natural disasters in creating power outages is more significant. The occurrence of natural disasters such as hurricanes, floods, earthquakes, and low-probability high-impact (LPHI) events can raise extreme damages to power systems, the number and severity of which have been increasing in recent years [1,2]. In case of a disaster, restricting the range and duration of the outage is a crucial action. Considering the many consequences of power outages, the resilience of a power grid to natural hazards is essential [3]. Resilience in power grids is defined as the ability to mitigate the vulnerability of a system faced with LPHI events [4]. Resilience is a time-dependent concept that must be considered before, during, and after a severe disaster to enhance it. The risk and vulnerability evaluation of customers affected by the disruption is required to assess power systems' resilience. Previous studies have addressed the impact of natural disasters on the risk of power outages and response to these events by one of statistical, structure-based, and fragility curves-based models [5].

Statistical-based models are widely used by utilizing historical data of atmospheric factors and system damages [6]. However, these models are sometimes not easily generalizable due to a lack of information. On the other hand, structure-based models require the accurate implementation, complex simulations and modelling of generators, load points, substations, and transmission and distribution lines [7]. This model is very time-consuming as it relies on conducting complex power flow studies with high calculation burdens. Besides, the fragility curves-based models can estimate the probability and extent of damage to a power grid exposed to physical attacks [8]. But this model also requires a proper understanding of the intensity and type of natural events. Investigating severe weather events such as hurricanes for which historical data is available and using a simple structure-based model can determine the severity of the disaster for each point of the electrical system. Hence, with the help of fragility curves, the probability of

* Corresponding author.
E-mail address: aam@energy.aau.dk (A. Anvari-Moghaddam).

https://doi.org/10.1016/j.ress.2022.108536
Received 9 November 2021; Received in revised form 3 April 2022; Accepted 15 April 2022
Available online 18 April 2022

Nomenclature

Sets

Ω_B	Set of system buses.
Ω_G	Set of generators.
Ω_I	Set of Monte-Carlo iterations.
Ω_ℓ	Set of system lines.
Ω_S	Set of generated scenarios in each Monte-Carlo iteration.

Indices and Symbols

g	Index of generation units (1 to Ω_G).
i, j	Index of system buses (1 to Ω_B).
ij	Index of system lines (1 to Ω_ℓ).
τ	Index of Monte-Carlo iterations (1 to Ω_I).
ς	Index of generated scenarios in each Monte-Carlo iteration (1 to Ω_S).
ς'	Index of selected scenario in each Monte-Carlo iteration.
ς'	Feasible power flow set under natural disasters.
ς'	Uncertainty set of damaged components.
ς'	Feasible set for budget planning decisions.
$\overline{\cdot}, \underline{\cdot}$	Symbols for the upper and lower bounds of variables.

Parameters

B^{Total}	Total network planning budget (*M$*).
C_{ij}^{NH}	Hardening cost of line ij (*$/km*).
C_i^{MG}	MG installation cost in bus i (*$/MW*).
M	Large positive constant value.
P_i^D	Load demand at bus i (*MW*).
$\overline{P_g^G}/\underline{P_g^G}$	Upper and lower generation power limits of unit g (*MW*).
$\overline{P_{ij}^{\ell,critical}}$	Ultimate power of line ij.
$\overline{P_{ij}^{\ell,normal}}$	Rated power of line ij.
$\overline{P_i^M}$	Upper power limit of a MG at bus i (*MW*).
R^G	Number of generators attacked.
R^ℓ	Number of lines attacked.
T	Hurricane return period (*year*).
Z^{NH}	Number of defender's lines for hardening.
Z^{MG}	Number of defender's buses for MG placement.
n	Shape parameter for adjusting wind speed distribution.
r	Radial distance from the hurricane center (*km*).
x_{ij}	Reactance of line ij (*Ohm*).
z	Load ratio supplied by MGs.
δ_{ij}	Matrix connecting lines to buses.
α, μ	Weibull distribution function parameters.

Variables

f	The fraction of load affected by the severe disaster.
I_g	Commitment status of generator g.
$N(y)$	Normalization function in terms of y.
$\widehat{N}_{\varsigma,\tau}^{WpC}$	Criterion for selecting scenario ς' as the WpC of attack.
$\widehat{N}_{g,\varsigma,\tau}^{G}$	Impact of normalized wind speed on generator outage g in scenario$\varsigma$of iteration τ.
$\widehat{N}_{ij,\varsigma,\tau}^{\ell}$	Impact of wind speed and changes of power flow on the line outage ij in scenario$\varsigma$of iteration τ.
$\widehat{N}_{\varsigma,\tau}^{LS}$	Normalized load shedding in scenario$\varsigma$of iteration τ.
$P_i^{D,Hardened}$	Hardened load at bus i through resilience strategies (*MW*).
$P_i^{D,Connected}$	Connected load to non-faulted bus i (*MW*).
P_g^G	Generated power of unit g (*MW*).
P_{ij}^{ℓ}	Power flow of line ij (*MW*).
P_i^{LS}	Load shedding at bus i (*MW*).
$P_{i,\varsigma,\tau}^{LS}$	Load shedding at bus i and in scenario$\varsigma$of iteration τ(*MW*).
P_i^M	Generated power of MG at bus i (*MW*).
Pr_{ij}^{PF}	Failure probability of line ij caused by changes of power flow.
Pr_{ij}^{WS}	Failure probability of line ij caused by wind speed.
RM	Resilience metric.
$\overline{R}$	Maximum wind radius per moment (*km*).
VI	Vulnerability index.
v	Wind speed (*m/s*).
$\overline{v}$	Maximum wind speed per moment (*m/s*).
θ_i	Bus phase angle (*rad*).
χ_g	Binary variable for status of damaged generator g.
$\chi_{g,\varsigma/\varsigma',\tau}$	Binary variable for status of damaged generator g in scenario$\varsigma/\varsigma'$of iteration τ.
γ_{ij}^{A}	Binary variable for status of damaged line ij.
$\gamma_{ij,\varsigma/\varsigma',\tau}^{A}$	Binary variable for status of damaged line ij in scenario$\varsigma/\varsigma'$of iteration τ.
$\gamma_{ij}^{S_{NH}}$	Binary variable for status of line ij hardening based on existing strategies.
γ_{ij}	Binary variable general status of line ij in terms of hardening and disconnection or connection.
$\sigma_i^{S_{MG}}$	Binary variable status of MG placement in bus i based on existing strategies.
ω_i	Status of MG islanding in bus i.

Abbreviations

AD	Attacker-defender.
AD-RP	AD resilient planning.
DER	Distributed energy resource.
RES	Renewable Energy Source.
GAMS	General Algebraic Modeling System.
LPHI	Low-probability high-impact.
MG	Microgrid.
MIP	Mixed-integer programming.
NH	Network hardening.
RM	Resilience metric.
VI	Vulnerability index.
WpC	Worst possible case.

network components outage is calculated. This means that the models based on statistical, structure, and fragility curves complement each other. In the present study, a stochastic approach using a combination of these three models is developed to calculate the failure priority of transmission system components against hurricanes.

Power systems typically use the $N-1$ criterion as a security measure to reflect the concerns of a system for day-to-day operations, with N representing the total number of system components. This criterion states that the system should be designed in such a way that in a failure case of any individual component at any time, the system will provide the required capacities without interruption [9]. However, this security measure cannot cover the possible conditions for a case when different system components are damaged simultaneously; thus, it cannot guarantee the desired performance. To address the issue described above suitably, this paper uses a more accurate measure known as $N-k$ criterion to consider the simultaneous outage of k electrical components

[10]. Utilizing this criterion and its effect on system load shedding can make the vulnerability model richer.

In the existing literature, some studies on power systems' resilience can be found. In [11], a bi-level model based on Monte-Carlo simulation is developed to assess the system vulnerability in response to extreme weather events and prioritize vulnerable lines of a distribution network. In [12], an indicator based on rated load shedding is used to select the worst-case scenario of the hurricane based on the probability of outage of each line and the resulting load shedding. The proposed model in [13] considers components' vulnerability due to windstorms based on the fragility curve. The main objective is to create a day-ahead unit commitment precautionary plan to reduce load shedding caused by the outage of transmission lines due to storms. A three-level model is presented in [14] to increase system resilience through network hardening (NH) to maximize hurricane severity and worst-case lines interruption. The NH is one of the most effective ways to protect power systems from LPHI events [8]. There are various NH strategies such as upgrading the overhead structure, vegetation management, and a hybrid strategy based on integrating these two strategies. Reinforcement of the overhead structure is an initial NH strategy that involves upgrading the transmission poles to the higher class and renewing the power flow path. Extensive vegetation management can also help to harden the transmission system, as falling and breaking trees can cause power outages in severe storms [15]. In [16], an optimal NH operation is proposed to increase the strength of power systems. In that study, the pre-event resilience optimization measures are conducted to reduce the possibility of failure of distribution systems and load shedding.

In [17], microgrids (MGs) are introduced as promising solutions for improving the resilience of power systems. Moreover, the importance of installation and determining the boundaries of MGs in the occurrence of LPHI events is mentioned. Once a fault occurs, the MGs are separated from the upstream grid and operated independently. In this case, distributed energy resources (DERs) integrated into the MGs provide the required power for loads and prevent load shedding [18]. Various DERs, such as wind turbines, photovoltaic cells, controllable distributed generators, and energy storage systems can be integrated into MGs [19]. With the recent innovations in power system modernization, DERs are becoming more feasible to supply system demand in times of crisis. For instance, the energy storage system facilitates the use of distributed renewable generations. Also, it reduces the dependence of MG on the upstream grid by discharging the stored energy during power shortages [20]. In [21], a comprehensive review is provided of the use of MGs in providing network energy support.

Assessment of the resilience concept in power systems in dealing with LPHI events is time-dependent [22]. An appropriate metric should evaluate the impact of the resilience improvement strategies. Most articles use reliability indicators such as energy not supplied and the value of lost load to assess the resilience of electricity networks [11,17]. In contrast, there is a big difference between the concepts of resilience and reliability, which is fully addressed in [23]. In [24], the system infrastructure resilience is evaluated, and an indicator for operational resilience is presented in [25]. An appropriate resilience metric (RM) should be risk-based and able to take into account system vulnerabilities and the consequences of threats [26]. Spatio-temporal characteristics of a natural disaster are also crucial for resilience measurement in power systems [27]. A comprehensive criterion for assessing the power grid resilience should include the time dimension for operational and infrastructural measures. The classification of studies in terms of the system vulnerability and grid protection to improve resilience is given in Table 1.

In the reviewed studies, providing a comprehensive vulnerability model based on the available tools has received little attention. It means there are no proposed vulnerability models that include all items of attacker statistical assessment, topological and electrical system evaluation, and observation of threat consequences. Besides, existing studies have mainly used reliability indexes such as expected energy not being used to assess resilience. Also, the articles that used the RM have not included joint operational and infrastructural resilience in the metric. Therefore, a new RM should be considered in evaluating resilience, given this existing gap. According to the literature review, it can be concluded that a considerable part of the investigations on the power system resilience has concentrated only on vulnerability assessment or resilience enhancement strategies. In contrast, the effectiveness of a vulnerability evaluation and resilience improvement strategies are determined together. Also, it is worth noting that the previous studies have utilized one of the operational or infrastructure-related strategies to improve resilience.

This paper considers two measures of vulnerability analysis and system protection against an attacker to fill the gap above. Simultaneous consideration of these two approaches requires a correct and accurate understanding of how the threat affects the performance and efficiency of the transmission system. In this way, a linear two-stage model based on attacker-defender (AD) strategies (called AD-RP hereafter) is presented to model network vulnerability and outage mitigation. Attackers are natural disasters that can cause extreme damage to the power system. In contrast, defenders are actions that minimize the system's vulnerability against attacks. In the first stage, a novel vulnerability index (VI) is introduced by a stochastic model based on Monte-Carlo

Table 1
The taxonomy of references based on the assessment of vulnerability and resilience.

Section	Description	Reference Number [4]	[7]	[25]	[10]	[11]	[12]	[13]	[14]	[15]	[16]	[23]	**This paper**
Vulnerability Assessment	Vulnerability index		✓			✓	✓	✓					✓
	Statistical features of the disasters		✓	✓			✓	✓			✓		✓
	Length and loading of power lines			✓		✓							✓
	Fragility curve-based		✓	✓		✓	✓	✓					✓
	Worst case	✓			✓	✓	✓	✓	✓		✓		✓
Resilience Assessment	Prior to an Event					✓			✓			✓	✓
	During an Event	✓	✓		✓	✓	✓	✓		✓	✓	✓	✓
	After an Event		✓	✓						✓		✓	✓
	System infrastructure												✓
	Load shedding	✓	✓		✓	✓	✓	✓	✓	✓	✓	✓	✓
	Resilience metric	✓		✓									✓
Resilience Improvement	Operational strategy	✓			✓	✓	✓	✓		✓		✓	✓
	Infrastructural strategy		✓	✓	✓				✓	✓	✓		✓

simulation in such a way the worst possible case (WpC) of components failure is presented. In the stochastic model, the impact of attack severity on the vulnerability of system components, length and loading of power lines, and load shedding are considered to model the worst possible attacker. In the second (defense) stage, the system resilience is improved using optimal MG placement (as an operational strategy) and NH (as an infrastructural strategy) based on the VI and considering budget constraints. Eventually, an innovative RM is presented to evaluate the proposed AD-RP model performance against the hurricane. This new metric involves the main properties of the resilience concept in electrical power systems. The major contributions of this paper are presented below.

- Developing an AD optimization model for vulnerability assessment and resilient planning in transmission power systems.
- Introducing a novel VI for selecting the WpC of electrical components outage.
- Considering the natural phenomenon severity, the length and loading of power lines, and load shedding in vulnerability analysis to model the worst possible attacker.
- Introducing a unique RM for evaluating the system performance, including all resilience concept attributes.
- Presenting an efficient defense planning for joint the operational and infrastructure-related strategies to cope with the transmission system requirement in an LPHI condition.

This paper is organized as follows: Section 2 describes the vulnerability assessment of the AD-RP model. The resilience assessment and presentation of the novel RM is presented in Section 3. The linear two-stage model mathematical formulations are given in Section 4. Section 5 provides simulations and numerical results. Finally, concluding remarks are presented in Section 6.

2. Vulnerability assessment

One aspect of resilience studies is the evaluation of system damage against the maximum severity of a threat. Severe weather events can make a significant impact on power grid components. In this paper, to model the outages caused by the occurrence of the natural phenomenon, a VI for selecting the critical components is presented. The proposed VI is calculated based on combining the WpC of attack, disaster statistical analysis, system structure, and fragility curves, as shown in Fig. 1.

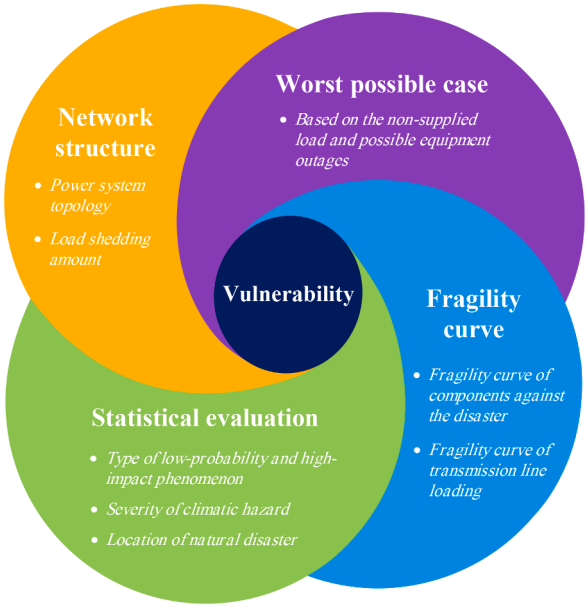

Fig. 1. The considered elements for VI calculating.

2.1. Worst possible case

The vulnerability assessment model uses the $N - k$ criterion to determine the priority order of damage to electrical components. A stochastic model is used to determine the extent of components' vulnerability, and a probabilistic method is also assumed for the natural disaster. The $N - k$ criterion guarantees the system's resilience to the outage of k components from the set of elements within the affected area. It is also noteworthy that if k components are damaged, there will be a lot of possible failure scenarios (N choose k). Since evaluating all possible scenarios is a challenging issue, it is required to consider the worst possible scenario. Accordingly, the scenarios of components outage must be chosen that lead to the WpC of attack. In this approach, the factors, including the impact of the hurricane on the power equipment outages and load curtailment, are used to determine the WpC of the disaster. Consequently, a scenario of outages must be selected, including the most amount of wind speed on the damaged lines and generators and leading to the most load shedding. The method of calculating the VI and selecting the WpC of outages has been developed in Section 4.

2.2. Disaster statistical analysis

In this paper, a model based on statistical analysis is developed to figure out the spatial and temporal dynamics of natural disasters. Here, resilience studies are carried out against the hurricane threat. A critical value theory is used as a suitable technique to calculate the maximum wind speed values. Critical value theory presents the occurrence of a hurricane in the form of probabilistic distributions by studying the trend of historical data occurrence and repeating maximum values (and minimum values in some natural phenomena). In other words, the critical value theory states that in a return period T, the occurrence of a hurricane with an estimated speed v is expected [11].

Hurricanes research and simulation confirm that the Weibull distribution is appropriate for predicting hurricane wind speeds. The two-parameter Weibull cumulative distribution function is given by Eqn (1):

$$F_v(v) = 1 - \exp\left[-\left(\frac{v}{\mu}\right)^{\alpha}\right] \tag{1}$$

where the dispersion and scale parameters, α and μ, are site-specific. These two parameters define the relationship between the wind speed and return period in Eqn (2):

$$v = u\left[-\ln\left(\frac{1}{T}\right)\right]^{\frac{1}{\alpha}} \tag{2}$$

The authors in [28] have shown the peak wind speeds at the return periods of 50, 100 and 1000 years are 132, 150 and 182 mph (58, 67 and 85 m/s), respectively. These values are obtained based on the Weibull parameters μ=61.07 and α=1.769 for south Florida. This means that as the return period grows, the hurricane velocity increases. Therefore, estimating wind speed according to the critical value theory is necessary to assess the risk of electrical equipment.

Based on a hurricane's spatial and temporal dynamics, it is assumed that when a hurricane enters an area, floods and strong winds make a greater impact on power system components close to the shoreline. A hurricane as one of the most well-known natural disasters decreases in intensity and speed when it lands on its path [29]. As Fig. 2 implies, after the hurricane landed and entered the land area, the wind speed is gradually decreased over time, and at the same time, its impact radius is increased. Due to the fragility curve, the probability of component failure also becomes smaller as wind speed decreases. Hence, the hurricane has little effect on distant power lines based on geographical locations.

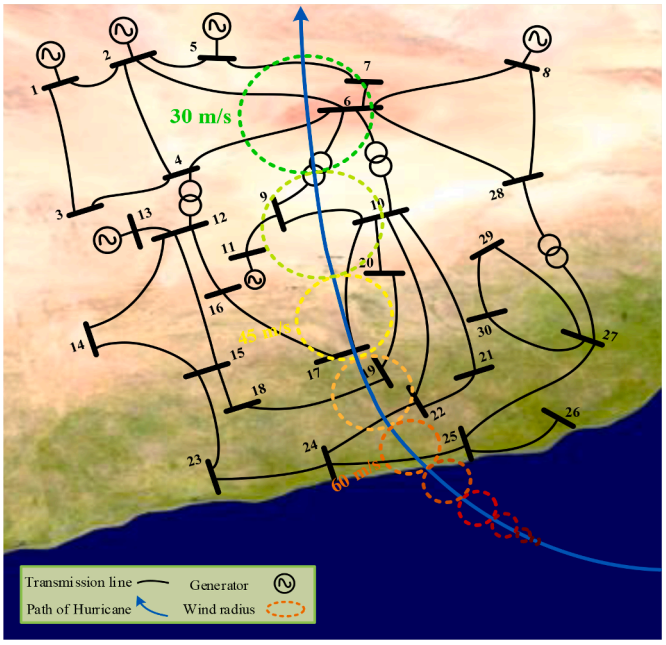

Fig. 2. The model of hurricane occurrence in the IEEE 30-bus transmission system.

The vortex model has been widely used to simulate hurricane occurrence. The modified vortex model assumes that concentric circles represent the wind flow in a fixed and ideal tropical hurricane. In this model, the wind speed in the centre is equal to zero. The wind speed reaches steeply to its topmost value at the maximum radius and then decreases to zero by increasing the radius [30]. The wind speed distribution in the modified vortex model is expressed by Eqn (3):

$$v_{ij} or v_g = \begin{cases} \overline{v}\left(\frac{r}{\overline{R}}\right)^n & r \le \overline{R} \\ \overline{v}\left(\frac{\overline{R}}{r}\right)^n & \overline{R} \le r \end{cases} \tag{3}$$

Where r is the radial distance from the storm centre, $\overline{R}$is the maximum wind radius, $\overline{v}$is the maximum wind speed at that moment, and n is the shape parameter adjusting the wind speed distribution [31].

2.3. System structure

To analyze the vulnerability of power systems, the structure and topology of the network need to be considered. The network components can be disconnected (damaged) or connected, and the location of their exposure to the hurricane is given in Fig. 2. It is shown in[11] that longer lines are more vulnerable among the power system lines. Thus, to determine the efficient VI, the distance between the components and the length of the transmission lines must be taken into account.

Moreover, components damaged by the attacker include generators and transmission lines. So disconnected network components cause load curtailment. That is, load shedding is one of the major factors to select the WpC of the disaster. Historical records demonstrate that the number of transmission lines and generators disconnected simultaneously does not exceed the number of lines attacked (R^{ℓ}) and the number of generators attacked (R^{G}), respectively [14]. Therefore, a stochastic set of uncertainties is introduced in Eqns (4), (5).

$$\mathbb{R} = \left\{ \sum_{ij \in \Omega_\ell} \gamma_{ij}^{A} \le R^{\ell}, \sum_{g \in \Omega_B} \chi_g \le R^{G}. \right\}, \forall ij \in \Omega_\ell, g \in \Omega_G, \left\{ \gamma_{ij}^{A}, \chi_g \right\} \in \{0,1\} \tag{4-5}$$

where two binary variables γ_{ij}^{A} and χ_g are used for the outage state of lines and generators, respectively. In these equations, A,$\ell$and g stand for attack, line and generator, respectively. It should be noted that if the lines and generators are disconnected, the value of both variables is 1; otherwise, the value is zero.

2.4. Fragility curves

In the traditional approach, the system outage and repair rate after an event is usually independent of the circumstances and time. While in the new approach, the components' vulnerability depends on weather conditions and loading [32]. The failure probability of transmission lines for varying wind speeds is shown in Fig. 3 (a). The failure probability of lines is different depending on weather parameters. Once some components are damaged in a disaster, the power flow through some lines may be changed or disrupted due to a significant change in the power supply. Similarly, the loading failure probability is obtained by mapping line load on the loading fragility curve. Fig. 3 (b) illustrates the linear relationship between the transmission line loading and the failure probability.

Strong winds can cause electrical poles to break, trees to fall on power lines, and other damage that affects and disables line performance. As shown in (3), the wind speed at the transmission line is obtained by its radial distance from the hurricane center. Each transmission line, based on its length, is divided into equal parts that the wind speed of each part is equal to its central wind speed. Hence the failure probability of part k in line ij due to the hurricane is expressed by Eqn (6):

$$\mathrm{Pr}_{ij}^{WS,k} = \begin{cases} 0 & 0 < v_{ij}^{k} < V_{des} \\ \exp\left[\frac{0.6931\left(v_{ij}^{k} - V_{des}\right)}{V_{des}}\right] - 1 & V_{des} < v_{ij}^{k} < 2\mathrm{V}_{des} \\ 1 & 2\mathrm{V}_{des} < v_{ij}^{k} \end{cases} \tag{6}$$

where $V_{des}$is the design wind speed of the transmission line, and $v_{ij}^{k}$is the wind speed of the center of part k in line ij [31].

The failure probability of the transmission line ij caused by wind speed consisting of K parts in a series is calculated by Eqn (7):

$$\mathrm{Pr}_{ij}^{WS} = 1 - \prod_{k=1}^{K}\left(1 - \mathrm{Pr}_{ij}^{WS,k}\right) \tag{7}$$

In case of damage to the transmission lines due to strong winds, the system topology changes and power is redistributed. Therefore, once the current of a line exceeds its rated capacity, its failure probability increases [31]. The failure probability due to power flow change is represented by Eqn (8):

$$\mathrm{Pr}_{ij}^{PF} = \begin{cases} \mathrm{Pr}_{ij}^{PF_0} & 0 < P_{ij}^{\ell} < \underline{P_{ij}^{\ell,normal}} \\ \frac{\left(1 - \mathrm{Pr}_{ij}^{PF_0}\right)\left(P_{ij}^{\ell} - \overline{P_{ij}^{\ell,normal}}\right)}{\overline{P_{ij}^{\ell,critical}} - \overline{P_{ij}^{\ell,normal}}} & \overline{P_{ij}^{\ell,normal}} < P_{ij}^{\ell} < \overline{P_{ij}^{\ell,critical}} \\ 1 & \overline{P_{ij}^{\ell,critical}} < P_{ij}^{\ell} \end{cases} \tag{8}$$

where $\mathrm{Pr}_{ij}^{PF_0}$denotes the probability of failure of line ij in normal weather conditions. In this paper, it is assumed that $\mathrm{Pr}_{ij}^{PF_0} = 0$. In other words,

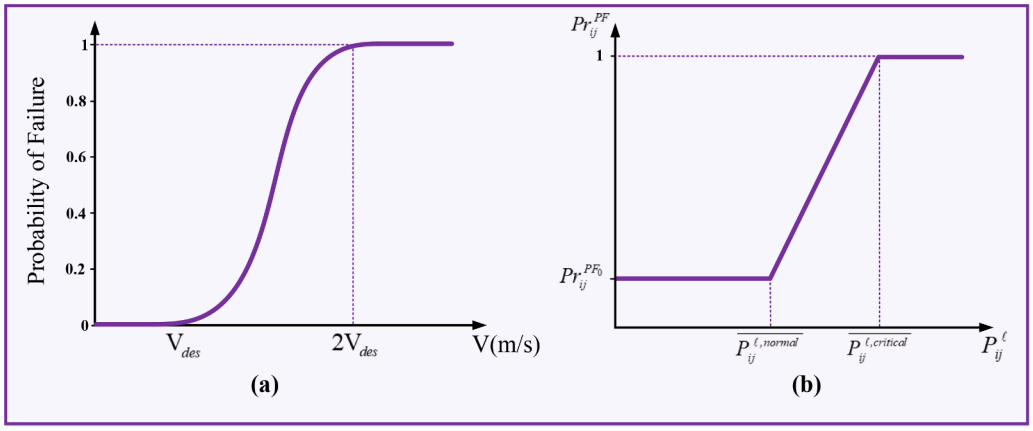

Fig. 3. Fragility curve: (a) related to transmission lines against varying wind speeds, (b) related to loading of power lines.

there is no failure probability in normal operating conditions. In addition, P_{ij}^{ℓ} represents the power of line ij, and $\overline{P_{ij}^{\ell,normal}}$ and $\overline{P_{ij}^{\ell,critical}}$ are rated and ultimate powers of line ij, respectively. The explanation how to combine the wind speed and the power flow changes together in the model is provided in Section 4.

To analyze the simultaneous effect of the system elements (such as the samples of wind speed and load shedding) on the VI of transmission network components, it is needed that the parameters be on a standard basis. The min-max normalization method is used to normalize the parameters to classify and compare these parameters fairly. Hence, the min-max normalization method is applied to normalize the parameters by Eqn (9):

$$N(y) = \frac{y - \underline{y}}{\overline{y} - \underline{y}} \tag{9}$$

where y can be wind speed or load shedding for instance. By using (9), the system parameters are normalized in a range of [0, 1]. In this model, to assess the vulnerability of lines, the severity of the hurricane, the length of the lines, and their loading are considered. Similarly, the severity of the hurricane for evaluating the vulnerability of generators is also assessed.

3. Resilience assessment

Assessing and determining the resilience of power systems is not a simple process, as resilience is a multidimensional concept with inherent complexities. Resilience indices are not standardized in the power system literature, and there is no general agreement on their capabilities and measurement methods. In this regard, there are countless indicators to assess resilience, but many of them examine only one or more aspects of the resilience concept. For instance, resilience is sometimes defined as the strength of a system's infrastructure against an attack. In some cases, it is interpreted as the operational activities required after a disaster or the grid recovery time after an LPHI fault.

According to Fig. 4 (a), the conceptual curve of resilience consists of five phases:

1) Pre-event: Disaster prediction and absorption.
2) Event progress: Breaking the grid resistance and increasing damages.
3) Post-event degraded: Self-organization considering resourcefulness.
4) Restoration: Getting back to the normal state through infrastructure recovery.
5) Post-restoration: Understanding new lessons from the event.

In order to assess resilience, Fig 4 (a) is considered. As can be seen, the ideal performance of the system is denoted by RM_{ideal}, which is a straight line here. When a disaster occurs in the network, the ideal performance level is reduced to a minimum resilience level RM_{Min} with a slope of $RM_{ideal} - RM_{Min}$. Finally, this performance index returns to the initial level assuming a linear recovery process. Thus, the system performance in the study period can be calculated by Eqn (10):

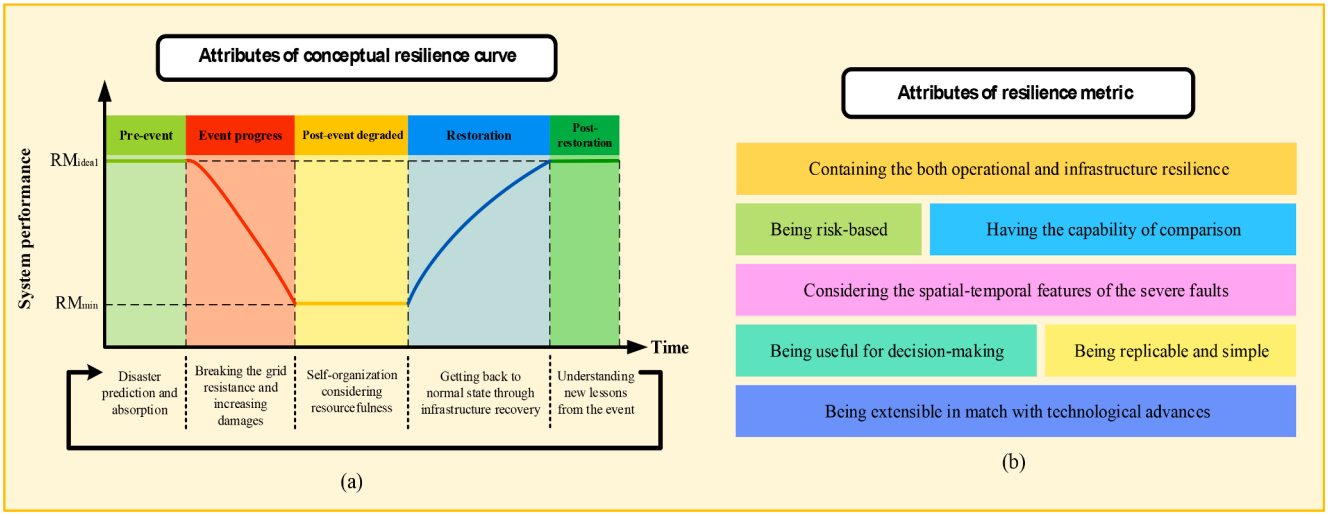

Fig. 4. The main features of (a) resilience curve and (b) RM.

$$Performance = \frac{\int_t RM(t)dt}{\int_t RM_{ideal}dt} \tag{10}$$

where $RM(t)$indicates the actual performance of the system at any given time.

It should be noted that the performance index always takes a value in the range [0, 1]. Using Eqn (10), the performance of the power system can be measured at different time intervals. The system performance index (vertical axis in Fig. 4 (a)) can be indicated by parameters such as the amount of loads shedding, the number of customers fed, the number of damaged components, and so on.

A unique RM is required to calculate the performance of the power system against severe weather events. In the context of resilience, a fraction of load affected by the LPHI events in Eqn (11) is considered. Where f is the ratio of the supplied loads (connected loads to non-faulted buses and hardened loads against the hurricane) to total the system loads (whether interrupted or non-interrupted). In this equation, $P_i^{D,Connected}$and $P_i^{D,\text{Hardened}}$indicate not-interrupted load against the hurricane before applying the resilience improvement strategies, and supplied load through the presented strategies, respectively. An appropriate RM should include all the attributes listed in Fig 4 (b) [33]. In addition to the affected loads, the proposed RM given in Eqn (12) includes both disconnected electrical components and the affected loads. That is, even if the equipment outages do not cause any load shedding, network resilience is still reduced. As the number of damaged components grows, the network's vulnerability and resilience decrease. Eventually, based on the obtained RM during the time, the power system performance is calculated by Eqn (10). To make the numerical answers tangible in evaluating the system's resilience and to facilitate the comparison of resilience levels of different cases, this metric is normalized between 0 and 1.

$$f = \frac{\sum_{i\in\Omega_B}\left(P_i^{D,Connected} + P_i^{D,Hardened}\right)}{\sum_{i\in\Omega_B} P_i^D} \tag{11}$$

$$RM = N\left(\frac{f}{e^{-f} + \log(R^{\ell} + R^{g})}\right), \quad \forall R^{\ell}, R^{g} > 0 \tag{12}$$

The system has sufficient power to supply the system loads in normal operation. If a natural disaster occurs, the affected area is disconnected from the main network. Under such circumstances, the affected area should be supplied with some alternative sources. Due to the limited budget, the NH and MG installation can be considered alternative operations to provide sufficient capacity to the affected area. It is assumed that sufficient funding is available to study the effectiveness of these infrastructural and operational strategies on system resilience during the hurricane. Hence, the budget set for the decision-maker can be adjusted by Eqns (13), (14):

$$\mathbb{Z} = \left\{ \sum_{ij\in\Omega_\ell} \gamma_{ij}^{S_{NH}} \le Z^{NH}, \right. \tag{13-14}$$

$$\left. \sum_{i\in\Omega_B} \sigma_i^{S_{MG}} \le Z^{MG}. \right\}, \forall i \in \Omega_B, ij \in \Omega_\ell, \left\{\gamma_{ij}^{S_{NH}}, \sigma_i^{S_{MG}}\right\} \in \{0,1\}$$

The equations show that the limited investment budget restricts the number of hardened lines and the installed MGs. The two binary variables $\gamma_{ij}^{S_{NH}}$ and $\sigma_i^{S_{MG}}$ are used for states of NH and MG placement in each bus, respectively. Once NH and/or MG placement is conducted, the value of both variables is equal to 1; otherwise, the value is zero. To show the number of defender's lines for hardening and the number of defender's buses for MG placement, Z^{NH} and Z^{MG} are used. According to the analysis of transmission line vulnerability and area type in terms of vegetation, two strategies are considered to increase resilience for NH. In the first one, the transmission poles are replaced with a higher class, and in the second one, in addition to upgrading the steel electric poles, the trees close to the transmission lines are trimmed. Besides, two strategies for the placement of MGs are also adopted. Both strategies are based on the suitability of the vulnerable areas for utilizing renewable energy sources (RESs). The area in the first one is not suitable for installing RESs, and diesel generators are used. In the second one, renewable distributed sources are mainly used to provide the required energy. Hence, in Eqns (13), (14), $S^{NH}$and $S^{MG}$are determined according to the aforementioned strategies.

In summary, the general framework of the proposed AD-RP model is shown in Fig. 5. Based on the vulnerability analysis performed for the probable event, the system planner decides which strategy to use to improve the system resilience. After applying each strategy on the power grid, feedback is taken from the information obtained to achieve the most optimal choice. Also, in this figure, the essential electrical and topological variables of the AD-RP model are presented.

4. Problem formulation

This section provides the mathematical formulation for optimal hardening of lines and optimal sizing and location of MGs. Minimizing load shedding for ensuring the resilience of the transmission network is the main objective behind the proposed model. According to the AD strategy, the proposed optimization problem is considered a linear two-stage model, shown in Fig. 6. In the first stage, known as the attack actions, the VI of system components is determined based on the most vulnerability of the transmission system against the hurricane. At this stage, a Monte-Carlo simulation based on a stochastic model for specific iterations is used to obtain the WpC for components outage due to the hurricane. In the second stage, as the defense operations, the operator minimizes load shedding caused by physical damage to network components while considering the budget constraints. The purpose is to obtain the optimal hardening of lines and optimal placement of MGs against WpC of hurricane events. Given that the proposed AD-RP model is a long-term and gradual planning model for the network, it must be constantly updated over time according to new standards and conditions.

The objective function associated with the first stage is formulated as Eqn (15). In each Monte-Carlo iterationτ, some scenarios (shown byς) are generated as attacks on the network equipment. After performing the power flow by minimizing the load shedding, the acceptable scenario in each iteration should be the most vulnerable attack. Eqn (16) is used as a criterion for selecting the worst attack among the scenarios generated in each iteration based on the normalized parameters. The load shedding parameter is normalized by Eqn (17). It states that the load curtailment at each bus can be within the range (0, 1). The effect of the normalized wind speed on the generator outage g is given by Eqn (18). Similarly, the impact of wind speed and changes of power flow on the line outage ij is given by Eqn (19). In this equation, it is assumed that the probability of the lines outages caused by the hurricane and changes of power flow are independent of each other.

$$\underset{q\in\mathbb{Q}(r)}{Min} \sum_{i\in\Omega_B} P_{i,\varsigma,\tau}^{LS} \tag{15}$$

$$\widetilde{N}_{\varsigma,\tau}^{WpC} = \widetilde{N}_{\varsigma,\tau}^{LS} + \widetilde{N}_{g,\varsigma,\tau}^{G} + \widetilde{N}_{ij,\varsigma,\tau}^{\ell}, \forall \varsigma \in \Omega_S, \tau \in \Omega_I \tag{16}$$

$$\widetilde{N}_{\varsigma,\tau}^{LS} = \sum_{i\in\Omega_B} N\left(P_{i,\varsigma,\tau}^{LS}\right), \quad \forall i \in \Omega_B, \varsigma \in \Omega_S, \tau \in \Omega_I \tag{17}$$

$$\widetilde{N}_{\varsigma,\tau}^{G} = \sum_{g\in\Omega_G} N(v_g).\chi_{g,\varsigma,\tau}, \forall g \in \Omega_G, \varsigma \in \Omega_S, \tau \in \Omega_I, \chi_{g,\varsigma,\tau} \in \{0,1\} \tag{18}$$

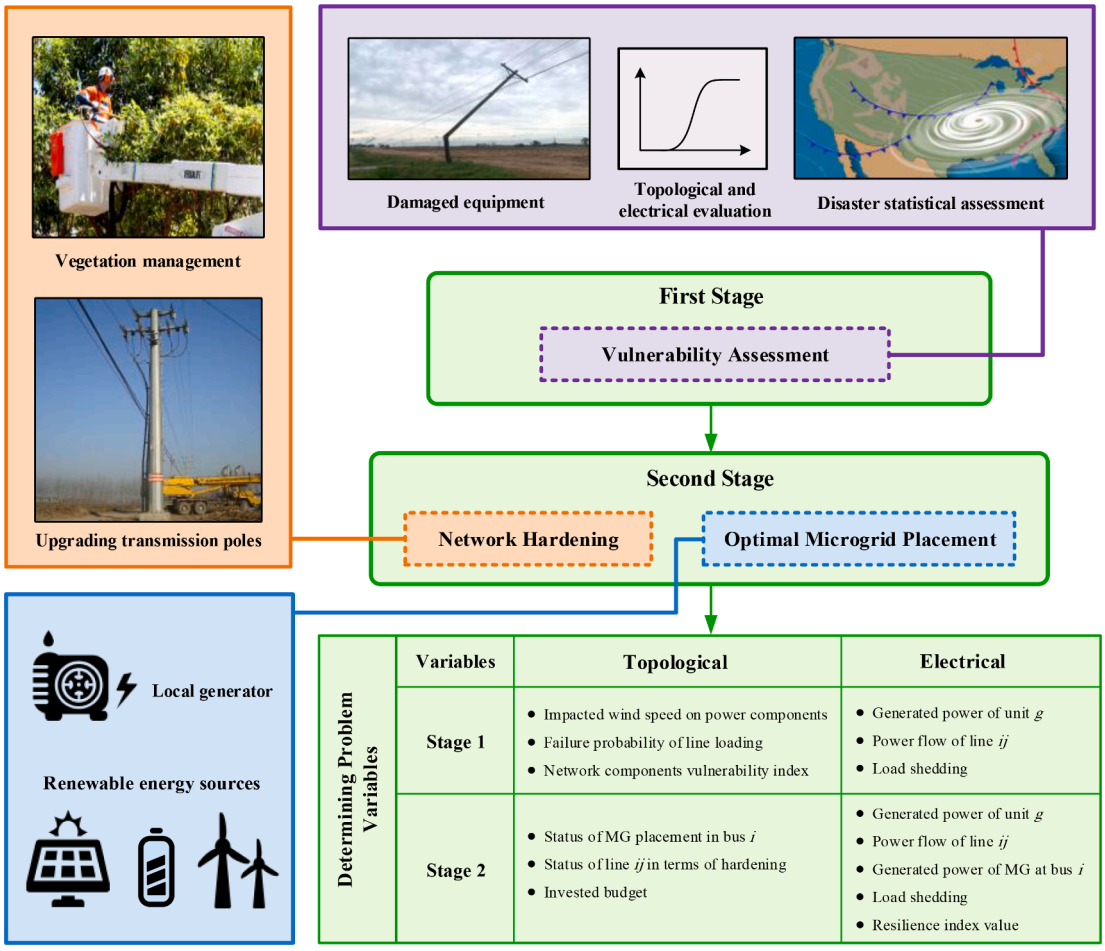

Fig. 5. The AD-RP model schematic for vulnerability analysis and improvement of transmission network resilience.

Fig. 6. The linear two-stage optimization problem based on the AD-RP model.

$$\widetilde{N}^{\ell}_{\varsigma,\tau} = \sum_{ij\in\Omega_{\ell}} \left(1 - \left[\left(1 - \mathrm{Pr}^{WS}_{ij}\right).\left(1 - \mathrm{Pr}^{PF}_{ij}\right)\right]\right).\gamma^{A}_{ij,\varsigma,\tau}, \forall ij \in \Omega_{\ell}, \varsigma \in \Omega_{S}, \tau \in \Omega_{I}, \gamma^{A}_{ij,\varsigma,\tau} \in \{0,1\} \quad (19)$$

The two binary variables $\gamma^{A}_{ij,\varsigma,\tau}$ and $\chi_{g,\varsigma,\tau}$ are for the outage state of lines and generators that are randomly generated ς times per each Monte-Carlo iteration. For binary values obtained from the components outage from all scenarios of each iteration, acceptable scenario lead to the maximization of normalized parameters. This means that if Eqn (16) bears the highest value in the scenario ς', this scenario is chosen to calculate the VI. The process of choosing the selected scenario of equipment outage continues in all τ iterations. As Eqn (20), the VI indicates that each transmission network component is damaged how many times in all repetitions performed.

$$VI = \begin{cases} \sum_{\tau\in\Omega_I}\sum_{ij\in\Omega_\ell} \gamma^{A}_{ij,\varsigma',\tau}, & \forall ij \in \Omega_\ell, \varsigma' \in \Omega_S, \tau \in \Omega_I \\ \sum_{\tau\in\Omega_I}\sum_{g\in\Omega_G} \chi_{g,\varsigma',\tau}, & \forall g \in \Omega_G, \varsigma' \in \Omega_S, \tau \in \Omega_I \end{cases} \quad (20)$$

The calculation steps of this index based on the WpCs are shown in Algorithm 1.

After determining the VI of the network, the transmission system planner responds to the outages to get the minimum load interruption by considering the budget constraints and feasible power flow decisions defined by$q \in \mathbb{Q}(z,r)$. The mathematical formula of the objective function associated with the second stage is given by Eqn (21), and there are different constraints in the optimization process of the AD-RP model that should be satisfied. The constraints are expressed in Eqns (22)-(32).

$$\underset{z\in\mathbb{Z}}{Min}\ \underset{r\in\mathbb{R}}{Max}\ \underset{q\in\mathbb{Q}(z,r)}{Min} \sum_{i\in\Omega_B} P^{LS}_i \quad (21)$$

$$\sum_{ij\in\Omega_\ell} C^{NH}_{ij}\gamma^{S_{NH}}_{ij} + \sum_{i\in\Omega_B} C^{MG}_i \sigma^{S_{MG}}_i \le B^{Total}, \quad \forall ij \in \Omega_\ell, i \in \Omega_B, \left\{\gamma^{S_{NH}}_{ij}, \sigma^{S_{MG}}_i\right\} \in \{0,1\} \quad (22)$$

$$\sum_{g\in\Omega^i_G} P^G_g + P^M_i + P^{LS}_i - P^D_i = \sum_{j\in\Omega^i_\ell} P^\ell_{ij}, \quad \forall ij \in \Omega_\ell, i \in \Omega_B, g \in \Omega_G \quad (23)$$

$$\underline{P^G_g}(1-\chi_g)I_g \le P^G_g \le \overline{P^G_g}(1-\chi_g)I_g, \quad \forall g \in \Omega_G, \chi_g \in \{0,1\} \quad (24)$$

$$\left|P^\ell_{ij} - \left(\frac{\theta_i - \theta_j}{x_{ij}}\right)\delta_{ij}\right| \le M\gamma^A_{ij}, \quad \forall ij \in \Omega_\ell, \gamma^A_{ij} \in \{0,1\} \quad (25)$$

$$\left|P^\ell_{ij}\right| \le \overline{P^\ell_{ij}}(1-\gamma_{ij}), \quad \forall ij \in \Omega_\ell, \gamma_{ij} \in \{0,1\} \quad (26)$$

$$\gamma_{ij} = \left[1 - \gamma^A_{ij}\left(1-\gamma^{S_{NH}}_{ij}\right)\right], \quad \forall ij \in \Omega_\ell, \left\{\gamma^A_{ij}, \gamma^{S_{NH}}_{ij}\right\} \in \{0,1\} \quad (27)$$

$$\omega_i = \prod_{j\in\Omega^i_\ell} \left|\delta_{ij}\right|(1-\gamma_{ij}), \quad \forall i \in \Omega_B, ij \in \Omega_\ell, \gamma_{ij} \in \{0,1\} \quad (28)$$

$$\sigma^{S_{MG}}_i \ge \omega_i, \quad \forall i \in \Omega_B, \left\{\omega_i, \sigma^{S_{MG}}_i\right\} \in \{0,1\} \quad (29)$$

$$0 \le P^{LS}_i \le \left(1 - z\left(1-\sigma^{S_{MG}}_i\right)\right)P^D_i, \quad \forall i \in \Omega_B, \sigma^{S_{MG}}_i \in \{0,1\} \quad (30)$$

$$\overline{P^M_i} \le zP^D_i, \quad \forall i \in \Omega_B \quad (31)$$

$$0 \le P^M_i \le \overline{P^M_i}\left(1-\sigma^{S_{MG}}_i\right), \quad \forall i \in \Omega_B, \sigma^{S_{MG}}_i \in \{0,1\} \quad (32)$$

Eqn (22) illustrates that the total cost invested in the system cannot exceed the budget planned by the planner. Eqn (23) ensures that the sum of the total energy produced by the generators, MGs, and the injectable power from neighbouring nodes to each bus equals the load value in that bus. The production capacity of generation units is limited by Eqn (24), which can be zero depending on the state of commitment (I_g) and outage (χ_g). The line current is calculated in Eqn (25), and the line flow limit is given in Eqn (26) according to the line capacity and its outage state. In these equations, θ_i shows the phase angle of bus *i*, *M* is a large positive constant value and$\overline{P^\ell_{ij}}$represents the upper power flow limit of line *ij*. The general condition of line *ij* in terms of hardening and vulnerability is presented in Eqn (27). In this problem, in response to the network outage, the MG switches to the islanded mode. If any of the lines connected to the MG bus are damaged due to the hurricane, the MG will be disconnected from the network. Thus, the MG operation status is defined as the result of the line outage connected to the MG bus. Once the MG switches to islanded mode, the MG load will be zero from the operator's point of view. This means that the MG feeds the local load. As shown in Eqn (28), the MG installation possibility in each bus is defined by the outage state of the lines connected to that bus. ω_i illustrates the status of MG *i* (if *MG i* operates in an islanding model, the value is equal to zero; otherwise, it is 1) and $\delta_{ij}$is the matrix connecting lines to buses. Eqn (29) shows that the buses for MG installation should be selected among the permissible buses obtained from Eqn (28). Status of MG installation is demonstrated by $\sigma^{S_{MG}}_i$(if the MG is installed in bus *i*, the value is equal to 1; otherwise, it is 0). It is worth noting that the load shedding variable $P^{LS}_i$is set to zero in normal operation, and in critical operation, the amount of load shedding in bus *i* is limited by the load value, which the MG in that bus cannot supply. If the MG is not installed in bus *i*, the load shedding can be equal to the total load on bus *i*. Eqn (30) states that if the MG is not connected to bus *i*, the load shedding is limited to the total load value of that bus. Load ratio supplied by MGs is illustrated with *z*. As Eqn (31) implies, the power capacity of the MG installed in each bus is limited by the predetermined maximum load ratio in that bus. If any of the lines connected to the MG bus are damaged, the MG operation mode is set to zero. This means that the MG operates in an islanded mode. Given Eqn (32), by switching to islanded mode, the MG load will be zero from the viewpoint of the system operator, so the MG has to supply its own predicted load as zP^D_i.

Algorithm 1
Calculation steps of VI

1:	Initialization: $R^\ell, R^G \leftarrow$ Set to the specified value,
2:	$VI_{ij}, VI_g \leftarrow$Set to zero for all the network components,
3:	$\tau, \varsigma \leftarrow$ Set iteration indexes to the specified value;
4:	**while** (τ)
5:	**for** (ς)
6:	**Generate:** $\gamma^A_{ij,\varsigma,\tau}, \chi_{g,\varsigma,\tau} \leftarrow$Stochastic binary in scenario ς;
7:	**Solve:** Objective function;
8:	**end for**
9:	**Select:** Maximum value of $\widehat{N^{WpC}_{\varsigma,\tau}}$ in scenario ς',
10:	if$\gamma^A_{ij,\varsigma',\tau} = 1 \leftarrow VI_{ij} = VI_{ij} + 1$,
11:	if$\chi_{g,\varsigma',\tau} = 1 \leftarrow VI_g = VI_g + 1$;
12:	**end while**
13:	**Output:** *VI*

5. Numerical Results

This section applies the proposed AD-RP model to the IEEE 30-bus transmission system, and the simulation results are provided and discussed. Fig. 2 depicts the test system, which comprises 6 generators and 41 lines. The length of transmission lines of the test system is shown in Fig. 7 [34]. The parameters of the Weibull distribution in a 50 year return period under climatic conditions given in [11] are chosen as μ=61.07 and α=1.769. Therefore, the wind speed is obtained as 60 m/s at the moment of entering the land and it is assumed that after landing the speed is reduced to 30 m/s. The wind speed interpolates between the points based on Eqn (3). The hurricane-force wind can extend outward from 185 to 555 km [35]. For modelling the failure probability of transmission lines, every 10 km is divided into one part. Also, $V_{des}$is assumed 30 m/s for all transmission lines. The shape parameter adjusting the wind speed distribution is often set within the range$0.4 < n < 0.6$. The load ratio provided by the MGs as *z* is considered to be 30%. The parameters related to the capacity of lines as $\overline{P^{\ell,normal}_{ij}}$ and $\overline{P^{\ell,critical}_{ij}}$ are considered as 1.170 and 0.87, respectively [31]. The investment budget limit is regarded as 70 $M [36]. The distance between the poles is assumed to be 350 m, and each transmission line contains several steel poles according to the length of that line. As mentioned earlier, for both NH and MGs placement, two strategies are considered. The input information to the proposed problem for IEEE 30-bus test system based on the resilience improvement strategies is shown in Table 2. After hardening the lines based on the strategies of upgrading the pole class and vegetation management, it is assumed that the hardened lines are resistant to wind speeds of 0 to 60 m/s. It is

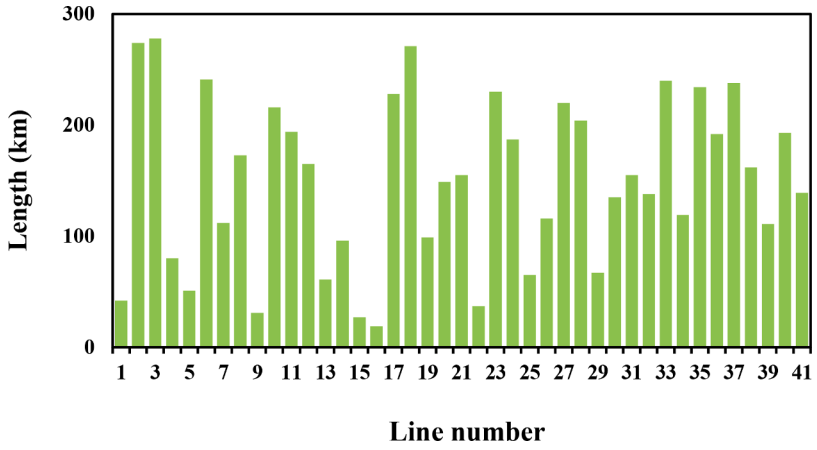

Fig. 7. The length of transmission lines in the IEEE 30-bus test system.

Table 2
The costs and corresponding lines and buses based on resilience improvement strategies

	Strategy	Cost	Proper line/bus
Lines	1	7,500 ($/km)	L1, L2, L3, L4, L5, L6, L7, L8, L9, L10, L11, L12, L13, L14, L15, L16, L17, L18, L25, L40 and L41.
	2	11,000 ($/km)	L19, L20, L21, L22, L23, L24, L26, L27, L28, L29, L30, L31, L32, L33, L34, L35, L36, L37, L38 and L39.
Buses	1	0.6 (M $/MW)	B4, B6, B7, B8, B10, B15, B17, B18, B19, B21, B22, B23, B24, B25, B26, B27 and B30.
	2	1.5 (M $/MW)	B1, B2, B3, B5, B9, B11, B12, B13, B14, B16, B20, B28 and B29.

assumed that all components are online before the disaster occurs and the hurricane hits the network at 50 h from the beginning of the simulation (Pre-event phase). The duration of the hurricane is 24 hours (Event progress phase), and the post-event degraded phase takes 50 h. It is assumed that the time to repair each line is 20 h and to restore each MW is 8 h (Restoration phase). The simulation continues up to 24 h after the system is fully restored to a normal state (Post-restoration phase). The proposed optimization model is a mixed-integer programming (MIP) problem, which is simulated in the well-known General Algebraic Modeling System (GAMS) commercial software package and solved with CPLEX solver. The CPLEX is a GAMS solver for solving the MIP models. The AD-RP model has been executed in a PC with Intel Core i7 CPU @3.20 CPU and 4 GBs of RAM.

According to the vulnerability analysis and simulation of the first stage of the proposed AD-RP model, the results of the VI for 41 lines and 6 generators of the transmission system from the most vulnerable to the most resistant component are given in Fig. 8, respectively. As can be seen, the vulnerability of transmission system components is reduced from hot colours to cool colours. The elements with the red colour are the most vulnerable, and the components with the purple colour have the highest resistance against the modelled hurricane.

In the second stage of the AD-RP model, hardening of vulnerable lines and optimal placement of MGs are conducted according to the $N-k$ criterion. By increasing k according to the VI, the NH process and installation of MGs continue until the budget condition is met. In the following, three cases are performed and analyzed to examine the performance of the operations used in the proposed problem. The first one considers a case where only the NH is performed. The second one investigates a case where only the MG placement is performed. In the last one, both NH and MG placement are carried out simultaneously. It should be noted that the calculations of the RM are for the post-event degraded phase.

Case1: *Network resilience improvement by using NH*

This case provides the results of the hardening of transmission system lines on disrupted loads based on component VI. It is assumed that 18 components of the system are disconnected. This means that the NH is done according to the *N – 18* criterion. In Table 3, a summary of the results related to the performance of the NH is presented. Based on this

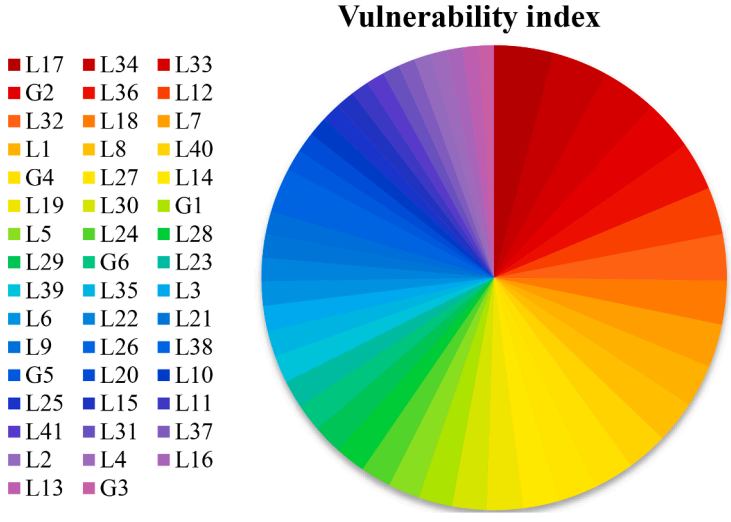

Fig. 8. VI for the component of the IEEE 30-bus system.

Table 3
Results of the system performance in response to components outage by optimal NH.

k	Initial *RM*	Hardened line	Strategy	Total hardened line length (km)	Total hardening cost (M$)	Final *RM*
1 to 2	1	L34	2	119	3.859	1
3 to 5	0.93 to 0.87	L36	2	311	10.081	1 to 0.95
6 to 8	0.84 to 0.81	L18	1	582	15.886	0.95 to 0.88
9 to 10	0.78 to 0.77	L1	1	624	16.786	0.88 to 0.86
11	0.75	-	-	624	16.786	0.85
12 to 13	0.72	L7	1	736	19.186	0.85 to 0.83
14 to 15	0.69 to 0.68	L14	1	832	21.241	0.83 to 0.82
16	0.64	-	-	832	21.241	0.81
17 to 18	0.43	…	…	…	…	0.46
…	…	…	…	…	…	…
…	…	…	…	…	70	…

table, when the number of damaged components increases from 1 to 18, the initial RM decreases. Table 3 also shows this metric after the NH operations. Note that for *k=11*, no line is hardened. This means that the objective function (load shedding) has reached zero, and there is no need to harden the lines at all. At this point, the system is in good operational condition, while the reason for *RM=0.85* is the damaged infrastructure. It can be inferred that NH operations up to *N – 16* are efficient so that by using both NH strategies, the RM is improved in comparison with its initial value, and it will reach 0.81. However, the NH operation reaches a saturation point with the outage increase of components up to *N – 18*. In other words, although the total number of hardened lines increases with an increase in the invested budget, the RM does not change much compared to its initial value. In fact, with increasing hurricane intensity, NH strategies alone are not able to improve network resilience.

Case2: *Network resilience improvement by using MG placement*

In this case, the system resilience through the placement of the MGs is investigated. It is assumed that, as in the previous case, 18 components of the system are damaged. Table 4 lists the optimized numerical results of the MG placement. The results include the optimal buses for installing MGs and the total capacity and cost of the installed MGs. As the table implies, more MGs should be installed by increasing the number of damaged components. Thus, the total capacity of the MGs increases to compensate for the system's inability to supply loads properly. Since the MG placement possibility in each bus is dependent on the outage state of the lines connected to that bus, for *k=3 to 5* there is no appropriate bus for MG installation. The table also suggests that with the outage increase of components, the RM decreases compared to the previous case and this metric value increases in the case of *N – 18*. In other words, although applying NH strategies works better in fewer outages than the MG placement strategies, for the case with high outages (considering *N – 18* criterion), the optimal placement of MGs with the intended budget is more appropriate. In addition, in the *N – 18* mode, there is no longer a damaged bus suitable for MG installation to reduce load shedding. Thus the placement of MGs will be stopped before it reaches the budget constraint.

Case 3: *Network resilience improvement by using both NH and MG placement*

In this case, both infrastructural and operational strategies are conducted simultaneously to improve the system's resilience. Table 5 lists the comprehensive results related to the performance of the second stage of the AD-RP model. The results include the total length of the hardened lines, the total cost of NH, the optimal buses for installing MGs, and the total capacity and cost of the installed MGs. As can be seen, once the severity of the disasters is low, NH is a priority as it is much more efficient than MGs and costs less to invest. However, as the severity of the disaster increases and the generators of the transmission system are damaged, the network needs higher penetration of MGs to supply part of the loads. In this case, no MGs are installed up to *N – 16* mode, while afterwards, the MG allocation is preferred. Due to the budget constraint, the capacity of the installed MGs is also limited. Comparing the RM obtained here with case 2 shows that case 2 could only perform the same as case 3 against very severe disasters, while case 3 offers a good performance for all intensities.

According to Table 5, the required budget for the hardening of transmission lines is about 21M$, while the allocated budget for installing MGs is about 49 M$. This means that the hardening of transmission lines requires less funding than installing MGs in the power grid. The hardened lines and installed MGs for case 3 and the *N-18* contingency are shown in Fig. 9.

For results comparison, the RM obtained in different cases (without considering the budget constraint) after the operational recovery phase are compared and shown in Fig. 10. The figure also includes the value of the initial RM for a case where no operations (NH and MG placement) are carried out. As can be seen, case 1 demonstrates a more efficient approach toward resilience improvement than case 2 for hurricanes of moderate intensity. By contrast, case 2 offers better performance than case 1 for very severe hurricanes. However, it can be concluded that case

Table 4
Results of the system performance in response to components outage by optimal placement of MGs.

k	Initial *RM*	Bus with installed MG	Strategy	Total installed MG capacity (MW)	Total MG cost (M$)	Final *RM*
1 to 2	1	M26	1	1.05	0.630	1
3 to 5	0.93 to 0.87	-	-	-	0.630	0.93 to 0.87
6 to 8	0.84 to 0.81	M15	1	3.51	2.106	0.85 to 0.82
9 to 10	0.78 to 0.77	M24	1	6.12	3.672	0.79 to 0.78
		M14	2	7.98	6.462	0.79 to 0.78
		M2	2	14.49	16.227	0.79 to 0.78
		M10	1	16.23	17.271	0.79
		M23	1	17.19	17.847	0.79
11	0.75	M7	1	24.03	21.951	0.77
		M5	2	34.29	37.341	0.78
12 to 13	0.72	M26	1	43.29	42.741	0.76 to 0.75
14 to 15	0.69 to 0.68	M21	1	48.54	45.891	0.71
16	0.64	M16	2	49.59	47.466	0.67
17 to 18	0.43	M4	1	69.87	59.634	0.62 to 0.61
		M12	2	73.23	64.674	0.62

Table 5
Result of the system performance in response to components outage by optimal NH and placement of MGs.

k	Initial *RM*	Installed MGs		Total installed MG capacity (MW)	Hardened lines		Total hardened line length (km)	Total invested budget (M$)	Final *RM*
		No. of bus	Strategy		No. of line	Strategy			
1 to 2	1	-	-	0	L34	2	119	3.859	1
3 to 5	0.93 to 0.87	-	-	0	L36	2	311	10.081	1 to 0.95
6 to 8	0.84 to 0.81	-	-	0	L18	1	582	15.886	0.95 to 0.88
9 to 10	0.78 to 0.77	-	-	0	L1	1	624	16.786	0.88 to 0.86
11	0.75			0	-	-	624	16.786	0.85
12 to 13	0.72	-	-	0	L7	1	736	19.186	0.85 to 0.83
14 to 15	0.69 to 0.68	-	-	0	L14	1	832	21.241	0.83 to 0.82
16	0.64	-	-	0	-	-	832	21.241	0.81
17 to 18	0.43	M4	1	20.28	-	-	832	33.409	0.54 to 0.53
		M5	2	30.54	-	-	832	48.799	0.56 to 0.55
		M8	1	39.54	-	-	832	54.199	0.58
		M7	1	46.38	-	-	832	58.303	0.60
		M2	2	52.89	-	-	832	68.068	0.62 to 0.61
		M21	1	56.11	-	-	832	70	0.62

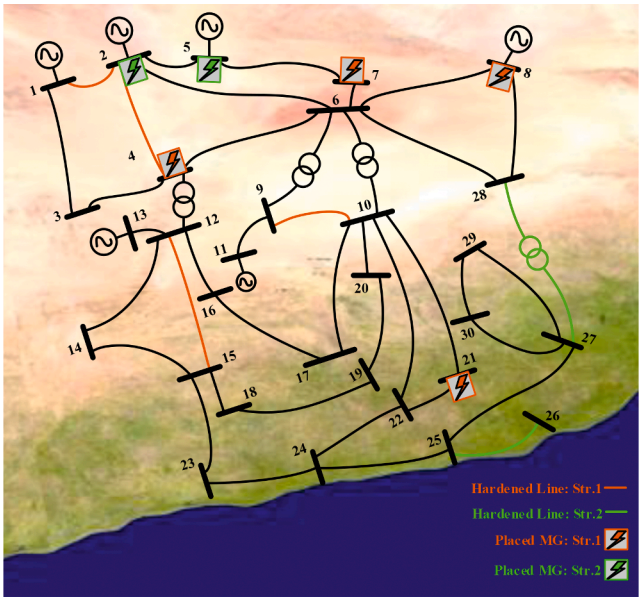

Fig. 9. Test system after NH and placement of MGs in case 3.

3 is more resilient than others as it gets the desired performance for all hurricane intensities.

In addition, the amounts of load shedding and investment budget after the operational recovery phase for different hurricane intensities are shown in Fig. 11. As the figure implies, the primary system's load shedding (without any operations) is impacted by an increasing number of damaged components. This is because no operations, including NH and MG placement, are implemented. By contrast, the capability and importance of the proposed model for network resilience improvement in the face of disruption are obvious, which significantly reduces the system load shedding. It is clear that as the wind speed increases, the network vulnerability raises, and naturally, more budget will be needed to reduce its consequences on the system.

5.1. The validity of the proposed model for a large-scale system

To verify the effectiveness of the proposed AD-RP model on large-scale systems, the model is applied to the IEEE 118-bus test system. The data of this system is given in [37]. The information on wind speed and its parameters, MGs allocation, and NH strategies are assumed to be the same in both test systems. Due to the larger system size in this section, it is assumed that the hurricane will land later and slow down along the way. After performing the vulnerability assessment, the hardened lines and installed MGs are presented in Fig. 12. The results are obtained for the conditions mentioned in case 3. It should be noted that operations and strategies to improve network resilience are applied based on vulnerable areas type in terms of vegetation and their suitability for utilizing RESs.

The calculated RM for the post-operational recovery phase without budget constraints is presented in Fig. 13 for different cases. As shown, the RM decreases with the increasing number of damaged components. The NH strategies in case 1 are more effective for low-intensity hurricanes. On the other hand, using the capacity of MGs installed in case 2 is more suitable for wider outages. Case 3 demonstrates that combining these two operations effectively improves resilience for all hurricane intensities and enhances the RM compared to cases 1 and 2.

5.2. Discussion

According to the definition of new RM presented, both load shedding and damaged system components are involved in evaluating network performance. Therefore, the results show that both infrastructure and operational strategies are necessary to increase the transmission system's resilience. In case 1, the NH operation has reached saturation point and could not further improve the RM with increasing the number of damaged components. In case 2, the capacity of installed MGs has recovered the part of load shedding, while the network is still very vulnerable due to the outages. Using both strategies simultaneously in case 3 improves the proposed metric for all $N - k$ criterion modes.

The system performance diagram is calculated based on each equipment's problem assumptions, recovery time, and all curve phases. The resilience curve associated with each case for $N - 24$ in the 33-bus test system is given in Fig. 14, in which the resilience metric is used to evaluate the system performance. The initial network means that no operations are conducted to improve the system's resilience. The

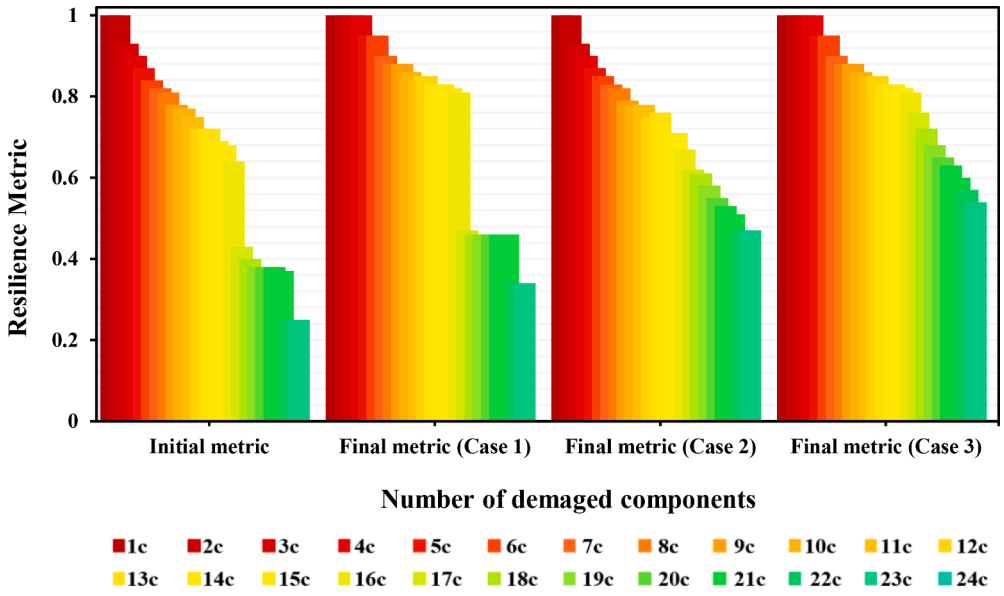

Fig. 10. RM after NH and MG placement without budget constraints.

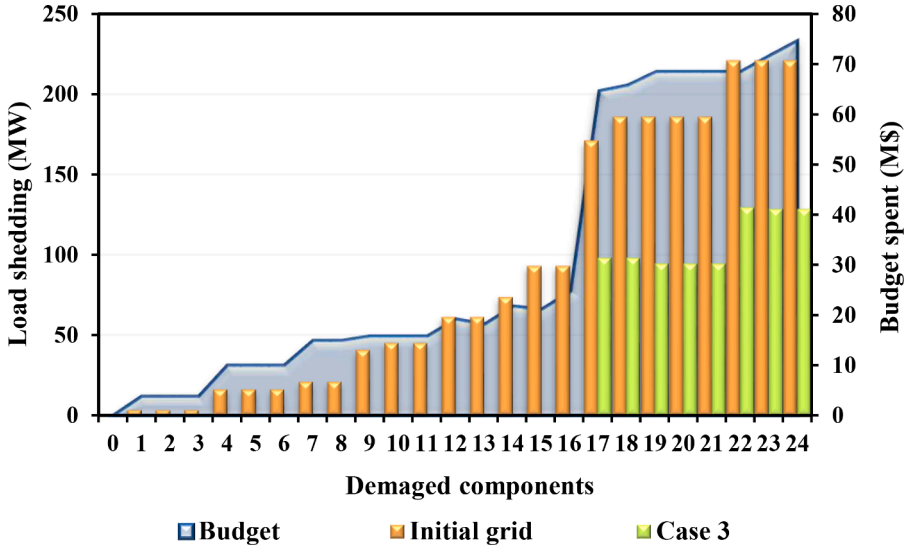

Fig. 11. Investment budget and load shedding for different hurricane intensities.

performance index of the studied system is approximately 0.63.

Due to the vulnerable transmission lines hardening in case 1, the performance index is not decreased as much as the initial network after the disaster. Since vulnerable and strategic lines became harder in the WpC, the remaining infrastructure restoration takes less time, and the performance index rises to 0.73. Utilizing the installed MGs in case 2 raises the performance index in the post-event degraded phase compared to case 1. While in the restoration phase, repairing network equipment in case 2 is not be as fast as case 1. The performance index in the second case is obtained as 0.72. Case 3, combining the strategies used in cases 1 and 2, yields an acceptable efficiency and improves the performance index to 0.83.

There is no doubt that any academic study can have strengths in various aspects and limitations. Therefore, the present study is no exception and has some limitations. The first limitation is the assumption of the linear relationship between the transmission line loading and the failure probability of lines. Moreover, another limitation of this paper is that the performance of the various parameters for calculating the VI is independent of each other. Also, as a proposal for future works and the continuation of this research, the benefits of different strategies can be compared, and a compromise between these measures and resilience improvement strategies can be established by cost-benefit analysis.

6. Conclusion

In this paper, a linear two-stage model based on AD strategies is proposed to improve the resilience of the electricity transmission network against the LPHI events such as a hurricane. In the first stage of the AD-RP model, a stochastic method was used to assess the vulnerability of system components based on wind speed, length and loading of power lines, and load shedding. A novel vulnerability index has been calculated to select the WpC of components failure. In the second stage, according to the conducted vulnerability analysis, optimal hardening of vulnerable lines and optimal placement of MGs are performed to enhance the power system resilience while considering the budget constraints. An effective, innovative RM was also introduced to evaluate the system's performance for the AD-RP model. The simulation results

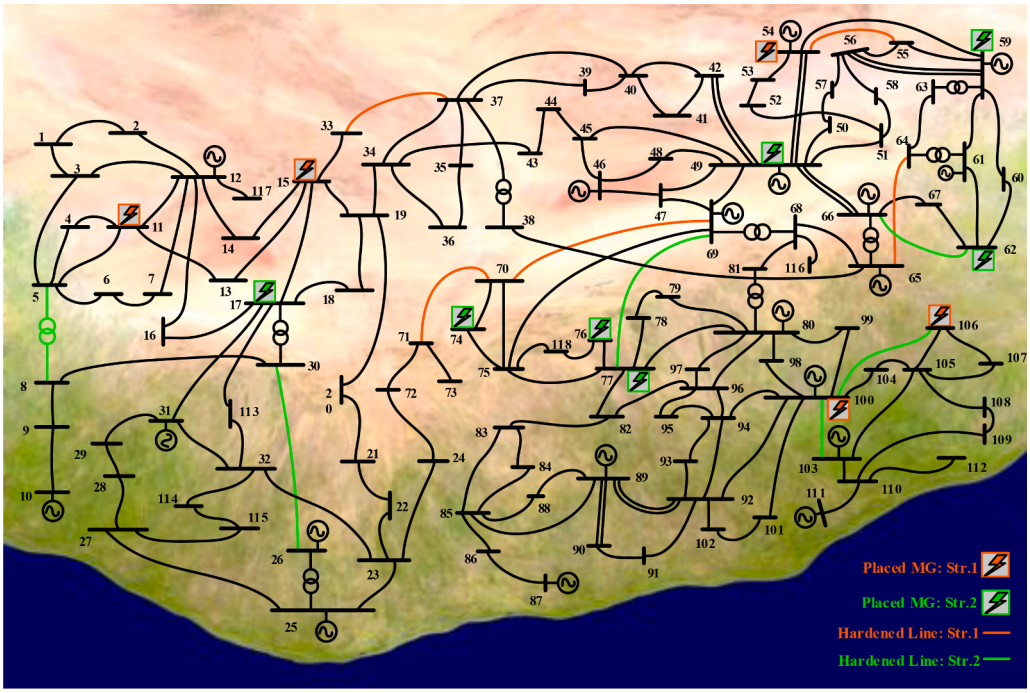

Fig. 12. The 118-bus test system after NH and placement of MGs in case 3.

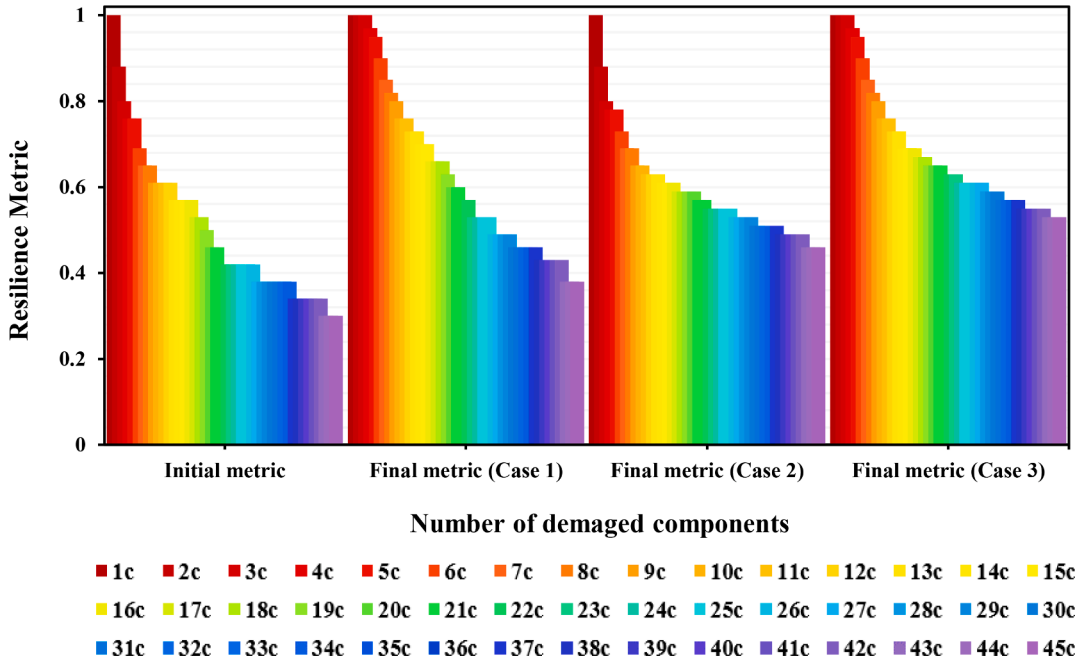

Fig. 13. RM after NH and MG placement without budget constraints in the 118-bus test system.

demonstrated the effectiveness of the proposed AD-RP model in increasing network resilience and highlighted the importance of two infrastructural and operational strategies for resilience improvement in the face of extreme natural disasters. The main conclusions of this paper are:

- Vulnerability assessment of transmission system components based on the worst possible attacker identifies the failure priority of transmission system components.
- Evaluation of system performance utilizing the proposed RM covers all phases of the resilience concept.
- NH strategies are effective in improving the transmission system performance against moderate-intensity hurricanes.
- The optimal placement of MGs is an essential action for the operational recovery phase of improving the system resilience.
- Both infrastructural and operational measures are required to raise the system's robustness and reduce the recovery time for the system's resilience enhancement.

CRediT authorship contribution statement

Kamran Jalilpoor: Conceptualization, Methodology, Software, Data

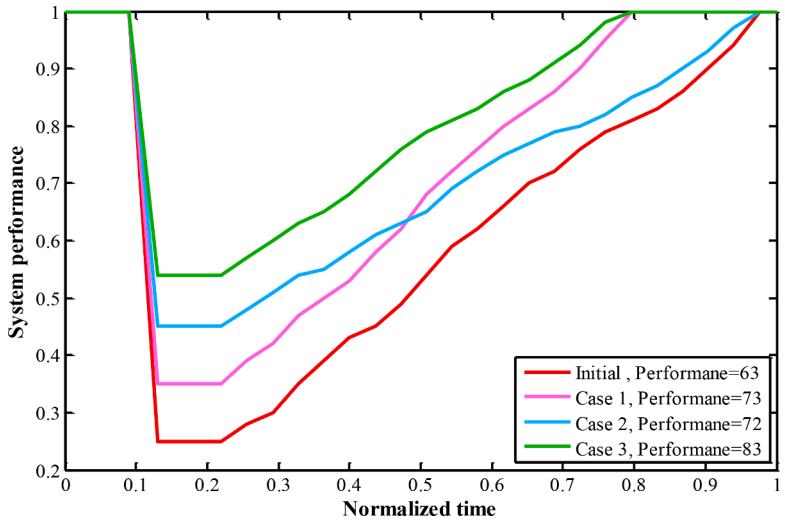

Fig. 14. Performance index calculated for different cases.

curation, Writing – original draft. **Arman Oshnoei:** Methodology, Software, Data curation, Writing – original draft. **Behnam Mohammadi-Ivatloo:** Methodology, Supervision, Writing – review & editing. **Amjad Anvari-Moghaddam:** Formal analysis, Methodology, Supervision, Writing – review & editing.

Declaration of Competing Interest

The authors declare that they have no known competing financial interests or personal relationships that could have appeared to influence the work reported in this paper.

References

[1] Wang J, Zuo W, Rhode-Barbarigos L, Lu X, Wang J, Lin Y. Literature review on modeling and simulation of energy infrastructures from a resilience perspective. Reliab Eng Syst Saf 2019;183:360–73.
[2] Zeng Z, Fang Y-P, Zhai Q, Du S. A Markov reward process-based framework for resilience analysis of multistate energy systems under the threat of extreme events. Reliab Eng Syst Saf 2021;209:107443.
[3] Shen L, Tang Y, Tang LC. Understanding key factors affecting power systems resilience. Reliab Eng Syst Saf 2021;212:107621.
[4] Aldarajee AH, Hosseinian SH, Vahidi B. A secure tri-level planner-disaster-risk-averse replanner model for enhancing the resilience of energy systems. Energy 2020;204:117916.
[5] Sperstad IB, Kjølle GH, Gjerde O. A comprehensive framework for vulnerability analysis of extraordinary events in power systems. Reliab Eng Syst Saf 2020;196:106788.
[6] Shen L, Cassottana B, Tang LC. Statistical trend tests for resilience of power systems. Reliab Eng Syst Saf 2018;177:138–47.
[7] Espinoza S, Poulos A, Rudnick H, de la Llera JC, Panteli M, Mancarella P. Risk and resilience assessment with component criticality ranking of electric power systems subject to earthquakes. IEEE Syst J 2020;14:2837–48.
[8] Hughes W, Zhang W, Bagtzoglou AC, Wanik D, Pensado O, Yuan H, et al. Damage modeling framework for resilience hardening strategy for overhead power distribution systems. Reliab Eng Syst Saf 2021;207:107367.
[9] Yang S, Chen W, Zhang X, Yang W. A graph-based method for vulnerability analysis of renewable energy integrated power systems to cascading failures. Reliab Eng Syst Saf 2021;207:107354.
[10] Zhang G, Zhang F, Zhang X, Wu Q, Meng K. A multi-disaster-scenario distributionally robust planning model for enhancing the resilience of distribution systems. Int J Electr Power Energy Syst 2020;122:106161.
[11] Khomami MS, Jalilpoor K, Kenari MT, Sepasian MS. Bi-level network reconfiguration model to improve the resilience of distribution systems against extreme weather events. IET Generat Trans Distrib 2019;13:3302–10.
[12] Nikkhah S, Jalilpoor K, Kianmehr E, Gharehpetian GB. Optimal wind turbine allocation and network reconfiguration for enhancing resiliency of system after major faults caused by natural disaster considering uncertainty. IET Renew Power Gener 2018;12:1413–23.
[13] Trakas DN, Hatziargyriou ND. Resilience constrained day-ahead unit commitment under extreme weather events. IEEE Trans Power Syst 2019;35:1242–53.
[14] Bagheri A, Zhao C, Qiu F, Wang J. Resilient transmission hardening planning in a high renewable penetration era. IEEE Trans Power Syst 2018;34:873–82.
[15] Ma S, Su L, Wang Z, Qiu F, Guo G. Resilience enhancement of distribution grids against extreme weather events. IEEE Trans Power Syst 2018;33:4842–53.
[16] Ma S, Chen B, Wang Z. Resilience enhancement strategy for distribution systems under extreme weather events. IEEE Trans Smart Grid 2016;9:1442–51.
[17] Najafi J, Peiravi A, Anvari-Moghaddam A, Guerrero JM. An efficient interactive framework for improving resilience of power-water distribution systems with multiple privately-owned microgrids. Int J Electr Power Energy Syst 2020;116:105550.
[18] Jalilpoor K, Ameli MT, Azad S, Sayadi Z. Resilient energy management incorporating energy storage system and network reconfiguration: a framework of cyber-physical system. Accepted to be published in IET Generation, Transmission & Distribution. 2022.
[19] Najafi J, Anvari-Moghaddam A, Mehrzadi M, Su C-L. An efficient framework for improving microgrid resilience against islanding with battery swapping stations. IEEE Access 2021;9:40008–18.
[20] Jalilpoor K, Khezri R, Mahmoudi A, Oshnoei A, Muyeen S, Islam S, et al. Optimal sizing of energy storage system. Chapter 2019;9:263–89.
[21] Hussain A, Bui V-H, Kim H-M. Microgrids as a resilience resource and strategies used by microgrids for enhancing resilience. Appl Energy 2019;240:56–72.
[22] Jalilpoor K, Nikkhah S, Sepasian MS, Aliabadi MG. Application of precautionary and corrective energy management strategies in improving networked microgrids resilience: a two-stage linear programming. Electric Power Syst Res 2022;204:107704.
[23] Ameli MT, Jalilpoor K, Amiri MM, Azad S. Reliability analysis and role of energy storage in resiliency of energy systems. Energy Storage in Energy Markets. Elsevier; 2021. p. 399–416.
[24] Fang Y-P, Sansavini G. Optimum post-disruption restoration under uncertainty for enhancing critical infrastructure resilience. Reliab Eng Syst Saf 2019;185:1–11.
[25] Sabouhi H, Doroudi A, Fotuhi-Firuzabad M, Bashiri M. Electrical power system resilience assessment: a comprehensive approach. IEEE Syst J 2019;14:2643–52.
[26] Poudel S, Dubey A, Bose A. Risk-based probabilistic quantification of power distribution system operational resilience. IEEE Syst J 2019;14:3506–17.
[27] Ma L, Christou V, Bocchini P. Framework for probabilistic simulation of power transmission network performance under hurricanes. Reliab Eng Syst Saf 2022;217:108072.
[28] Vickery P, Skerlj P, Twisdale L. Simulation of hurricane risk in the US using empirical track model. J Struct Eng 2000;126:1222–37.
[29] Xue J, Mohammadi F, Li X, Sahraei-Ardakani M, Ou G, Pu Z. Impact of transmission tower-line interaction to the bulk power system during hurricane. Reliab Eng Syst Saf 2020;203:107079.
[30] Chen W-B, Chen H, Hsiao S-C, Chang C-H, Lin L-Y. Wind forcing effect on hindcasting of typhoon-driven extreme waves. Ocean Eng 2019;188:106260.
[31] Guo J, Feng T, Cai Z, Lian X, Tang W. Vulnerability assessment for power transmission lines under typhoon weather based on a cascading failure state transition diagram. Energies 2020;13:3681.
[32] Panteli M, Mancarella P. Operational resilience assessment of power systems under extreme weather and loading conditions. In: 2015 IEEE Power & Energy Society General Meeting. IEEE; 2015. p. 1–5.
[33] Raoufi H, Vahidinasab V, Mehran K. Power systems resilience metrics: a comprehensive review of challenges and outlook. Sustainability 2020;12:9698.
[34] Deng F, Zeng X, Pan L. Research on multi-terminal traveling wave fault location method in complicated networks based on cloud computing platform. Protect Control Modern Power Syst 2017;2:1–12.

[35] McKinley K. Tropical storm and hurricane info, [online]. Available at https://www.oceannavigator.com/tropical-storm-and-hurricane-info/. 2014.
[36] Eskandarpour R, Lotfi H, Khodaei A. Optimal microgrid placement for enhancing power system resilience in response to weather events. In: 2016 North American Power Symposium (NAPS). IEEE; 2016. p. 1–6.
[37] Pena I, Martinez-Anido CB, Hodge B-M. An extended IEEE 118-bus test system with high renewable penetration. IEEE Trans Power Syst 2017;33:281–9.